Thermal diffuse scattering in grazing incidence diffraction

2003 J. Phys.: Condens. Matter 15 3367

(http://iopscience.iop.org/0953-8984/15/20/301)

INSTITUTE OF PHYSICS PUBLISHING JOURNAL OF PHYSICS: CONDENSED MATTER

J. Phys.: Condens. Matter **15** (2003) 3367–3374 PII: S0953-8984(03)58733-1

Thermal diffuse scattering in grazing incidence diffraction

S A Grigorian[1,3], J Grenzer[1], U Pietsch[1] and I A Vartanyants[2,3]

[1] University of Potsdam, Institute of Physics, Am Neuen Palais 10, 14469 Potsdam, Germany
[2] Department of Physics, University of Illinois, Urbana, IL 61801, USA
[3] Institute of Crystallography, RAS, Leninsky Prospekt 59, 117333, Moscow, Russia

Received 23 January 2003, in final form 7 April 2003
Published 12 May 2003
Online at stacks.iop.org/JPhysCM/15/3367

Abstract

Inelastic scattering of hard x-ray radiation by thermal phonons was studied by the x-ray grazing incidence diffraction technique. This method allows one to separate the contribution of the surface phonons from that of the bulk thermal excitations by tuning the penetration depth. It is shown that for smaller penetration depths the surface contribution to thermal diffuse scattering is approximately double the bulk one. The experimental results confirm the theoretical predictions derived from the Green function formalism.

1. Introduction

The processes of inelastic scattering of hard x-ray radiation have received increasing attention in recent years [1–3]. One such inelastic decay channel is the scattering of x-rays by thermal phonons: thermal diffuse scattering (TDS). The main features of TDS have been studied with synchrotron radiation using conventional the Bragg scattering technique in [4, 5]. Due to the large extinction length, surface effects could not be resolved. Moreover, in most of the previous works it was assumed that the main contribution to the processes of inelastic scattering of x-rays is due to the scattering by bulk acoustic modes of thermal vibrations. In recent papers the contributions of surface excitations to the total TDS signal [6, 7] were studied theoretically. It was predicted that surface TDS can make an important contribution to the total TDS yield if surface-sensitive scattering methods are used. The benefit of making surface-sensitive measurements combining grazing incidence diffraction (GID), x-ray reflectivity and x-ray fluorescence when investigating a perfect Ge crystal was demonstrated in [8].

In this paper we study surface and bulk TDS using GID. This technique has the advantage of allowing one to tune the penetration depth of the probing x-ray within the sample by means of the geometric conditions. Using an incident angle α_i smaller than the critical angle α_c, the penetration depth for x-rays is limited to about 10 nm, whereas for $\alpha_i \gg \alpha_c$, the penetration depth exceeds several hundreds of nanometres. Consequently, the sensitivity to the surface effects predominates in the first case. It will be shown that the surface TDS signal differs from

the bulk one. Of course, special care has to be taken in such experiments with the quality of the crystal and especially that of its surface.

2. Theory

The use of GID in the investigation of the near-surface properties of solids is well known. The general features of the GID method have been described elsewhere [9]. Under conditions of strong dynamical scattering, the TDS yield can be calculated in terms of general theory [10, 11]. The TDS yield $\kappa(\mathrm{TDS})$ for a perfect crystal and σ-polarized radiation can be obtained from the following expression:

$$\kappa(\mathrm{TDS}) = \sum_{i=1,2} \int_0^L \mathrm{d}z\, N_{TDS}(z) \times \{\mathrm{Im}[\chi_{00}]|D_0^i(z)|^2 + \mathrm{Im}[\chi_{hh}]|D_h^i(z)|^2 + 2\,\mathrm{Re}[D_0^{i*}(z)\,\mathrm{Im}[\chi_{0h}]D_h^i(z)]\}, \tag{1}$$

where the z-axis is directed into the crystal, L is the thickness of a crystal and $N_{TDS}(z)$ determines the probability yield of TDS at the surface of a crystal and where there are two incident ($D_0^i(z)$) and two diffracted waves ($D_h^i(z)$) inside the crystal corresponding to the two solutions of the fundamental equations of the dynamical diffraction theory [12] in GID geometry. Analysing the relationship (1), one can see that the shape of the function $\kappa(\mathrm{TDS})$ is essentially determined by the values of the imaginary parts of the susceptibilities $\mathrm{Im}[\chi_{00}]$, $\mathrm{Im}[\chi_{hh}]$ and $\mathrm{Im}[\chi_{0h}]$. These parameters are determined by geometric conditions, i.e. by the directions of the incident ($\boldsymbol{k}_0$), diffracted ($\boldsymbol{k}_h$) and inelastically scattered ($\boldsymbol{k}_g$) x-ray wavevectors, respectively. The two indices $0, h$ of $\mathrm{Im}[\chi_{0h}]$ indicate that the TDS is a function of two wavevector transfers, $\boldsymbol{K}_0 = \boldsymbol{k}_0 - \boldsymbol{k}_g$ and $\boldsymbol{K}_h = \boldsymbol{k}_h - \boldsymbol{k}_g$. This is in contrast to the case of Thomson scattering, where the dielectric susceptibility $\chi_{0,h}$ depends on a single scattering vector, $\boldsymbol{K} = \boldsymbol{k}_0 - \boldsymbol{k}_h$.

The amplitudes $D_{0,h}^{1,2}$ can be found from the fundamental equations of dynamical diffraction theory and the corresponding boundary conditions. In the following we consider σ-polarized radiation due to the chosen vertical diffraction geometry for the synchrotron measurements. After some straightforward calculations, one can obtain the following expression for the wave amplitudes inside a crystal [13]:

$$\begin{aligned} D_h^{1,2} &= \frac{2\alpha_i \chi_h (v_{2,1} + \alpha_f)}{[w_{1,2}(v_{2,1} + \alpha_i)(v_{1,2} + \alpha_f) - w_{2,1}(v_{1,2} + \alpha_i)(v_{2,1} + \alpha_f)]}\, E_0, \\ D_0^{1,2} &= -\frac{2[w_{1,2}(v_{1,2} + \alpha_f)(v_{2,1}^2 - \alpha_i^2) - w_{2,1}(v_{2,1} + \alpha_f)(v_{1,2}v_{2,1} - \alpha_i^2)]}{(v_{1,2} - v_{2,1})[w_{1,2}(v_{2,1} + \alpha_i)(v_{1,2} + \alpha_f) - w_{2,1}(v_{1,2} + \alpha_i)(v_{2,1} + \alpha_f)]} E_0, \end{aligned} \tag{2}$$

where

$$w_{1,2} = \frac{a}{2} \pm \sqrt{\frac{a^2}{4} + \chi_h \chi_{\bar{h}}}. \tag{3}$$

Here $a = -2(\theta - \theta_B)\sin 2\theta_B$ describes deviation from the exact Bragg conditions; α_i and α_f are the angles of the incident and diffracted waves, respectively. Using the Heaviside step function $\Phi(u_i)$, the parameters v_1 and v_2 in equation (2) can be written as

$$v_1 = u_1\Phi(\mathrm{Im}(u_1)) + u_2\Phi(\mathrm{Im}(u_2)), \qquad v_2 = u_3\Phi(\mathrm{Im}(u_3)) + u_4\Phi(\mathrm{Im}(u_4)), \tag{4}$$

where useful solutions are restricted to $\mathrm{Im}(u_i) \geqslant 0$. The following notation has been used in (4):

$$u_{1,2} = \pm\sqrt{w_1 + \alpha_i^2 + \chi_0}, \qquad u_{3,4} = \pm\sqrt{w_2 + \alpha_i^2 + \chi_0}. \tag{5}$$

The z-dependence of the x-ray wave fields $D_{0,h}^{1,2}(z)$ inside a crystal can be represented via solutions $v_{1,2}$ in the following form:

$$D_{0,h}^{1,2}(z) = D_{0,h}^{1,2} \exp(\mathrm{i}v_{1,2}k_0 z). \tag{6}$$

Here the amplitudes $D_{0,h}^{1,2}$ are given by (2) and we take into account that the diffraction vector lies parallel to the crystal surface.

Equations (1)–(6) can be used for the analysis of any kind of secondary process under GID conditions. In this case it is necessary to take into account the corresponding imaginary parts of the susceptibility and the probability of the secondary process considered in (1). Using the harmonic approximation, the imaginary part of the susceptibility that is responsible for inelastic scattering by thermal phonons can be written in a general form [14]:

$$\mathrm{Im}[\chi_{kk'}^{mn}] = \frac{(2\pi)^3 r_0^2 c}{\Omega_0 k^3} \sum_{\boldsymbol{k}_g} F^*(\boldsymbol{K}) F(\boldsymbol{K}') P^{mn}(\boldsymbol{k}_g) \times \left[\sum_{nn'} \mathrm{e}^{-\mathrm{i}\boldsymbol{K}\boldsymbol{R}_n + \mathrm{i}\boldsymbol{K}'\boldsymbol{R}_{n'}} Y(\boldsymbol{K}, \boldsymbol{K}', \boldsymbol{R}_n, \boldsymbol{R}_{n'}) \right] \delta(\omega - \omega_{k_g}). \tag{7}$$

In this expression the sum is over all unit cells and over all atoms in unit cells. The function $Y(\boldsymbol{K}, \boldsymbol{K}', \boldsymbol{R}_n, \boldsymbol{R}_{n'})$ is the correlation function of atomic displacements, $F_j(\boldsymbol{K})$ is the structure factor, $P^{mn} = (\delta^{ik} - k_g^m k_g^n / k^2)$ is the polarization tensor, r_0 is the classical electron radius, Ω_0 is the unit-cell volume. Here $\boldsymbol{k}$ and $\boldsymbol{k}'$ are equal to the wavevectors $\boldsymbol{k}_0$ or $\boldsymbol{k}_h$; $\boldsymbol{K} = \boldsymbol{k} - \boldsymbol{k}_g$ and $\boldsymbol{K}' = \boldsymbol{k}' - \boldsymbol{k}_g$ are the scattering vectors.

The most general consideration would take into account the scattering of the bulk phonons as well as the surface contribution to inelastic scattering. It has already been noted in a number of papers [4, 6, 10] that the main contribution to TDS in the scattering of hard x-rays is given by the long-wavelength acoustic modes. The optic branches contribute to a uniform background and therefore in our following consideration we will restrict ourselves to the contribution of acoustic branches only.

To take into account the influence of the surface effects explicitly, we will expand the general correlation function $Y(\boldsymbol{K}, \boldsymbol{K}', \boldsymbol{R}_n, \boldsymbol{R}_{n'})$ into two parts:

$$Y(\boldsymbol{K}, \boldsymbol{K}', \boldsymbol{R}_n, \boldsymbol{R}_{n'}) = Y^V(\boldsymbol{K}, \boldsymbol{K}', \boldsymbol{R}_n, \boldsymbol{R}_{n'}) + Y^S(\boldsymbol{K}, \boldsymbol{K}', \boldsymbol{R}_n, \boldsymbol{R}_{n'}). \tag{8}$$

Here the first term is responsible for the bulk contribution only and the second one for surface effects of all kinds.

The most effective way to consider these inelastic processes is to express the correlation function of atomic displacements in terms of the corresponding Green functions of the elasticity theory. Then, the Fourier components of the correlation functions [7] are

$$Y^V(\boldsymbol{K}, \boldsymbol{K}', \boldsymbol{R}, \boldsymbol{R}') = \left(\frac{k_B T}{8\pi}\right)\left(\frac{1}{C_{11}} + \frac{1}{C_{44}}\right)\frac{\boldsymbol{K}\boldsymbol{K}'}{|\boldsymbol{R} - \boldsymbol{R}'|}, \tag{9}$$

$$Y^S(\boldsymbol{K}, \boldsymbol{K}', \boldsymbol{R}, \boldsymbol{R}') = \left(\frac{k_B T}{8\pi}\right)\left(\frac{C_{11}^2 + C_{44}^2}{C_{11}C_{44}(C_{11} - C_{44})}\right)\frac{\boldsymbol{K}\boldsymbol{K}'}{\sqrt{(\boldsymbol{R} - \boldsymbol{R}')^2 + 4zz'}}, \tag{10}$$

where C_{11}, C_{44} and C_{12} are the three independent elastic moduli of a cubic crystal. As was noted above, the main contribution to TDS comes from acoustic phonons. Far from the surface, $z, z' \to \infty$, the contribution of $Y^S(\boldsymbol{K}, \boldsymbol{K}', \boldsymbol{R}, \boldsymbol{R}')$, equation (10), is becoming negligible compared to $Y^V(\boldsymbol{K}, \boldsymbol{K}', \boldsymbol{R}, \boldsymbol{R}')$, equation (9). From expressions (9) and (10) one can see that the bulk part depends only on the difference of the coordinates $|\boldsymbol{R} - \boldsymbol{R}'|$, whereas this is not the case for $Y^S(\boldsymbol{R}, \boldsymbol{R}')$. If we are interested in the contribution of long-wavelength excitations, the distance $|\boldsymbol{R} - \boldsymbol{R}'|$ is of the order of the acoustic wavelength λ_{ac}. The long-wavelength

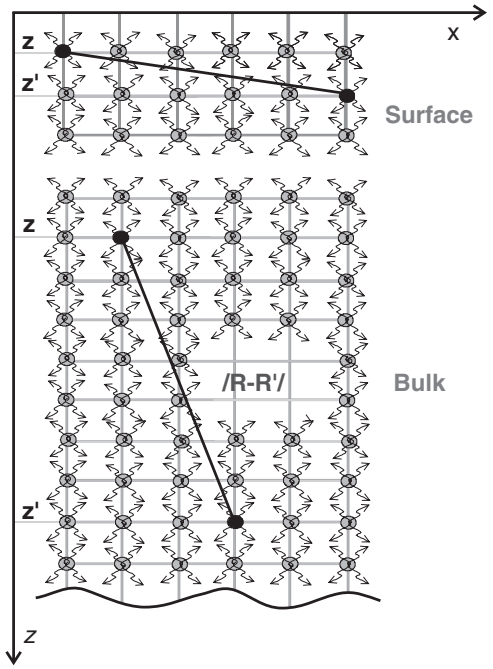

Figure 1. An illustration of the surface and bulk contributions to TDS.

acoustic waves propagating in a crystal have a range of wavelengths from a few nanometres to several tens of nanometres [15]. The contributions of surface and bulk thermal excitations are illustrated in figure 1. The thermal vibrations of the atoms in a crystal are shown. The black line connects two of those atoms over a distance $|\boldsymbol{R} - \boldsymbol{R}'|$; they have coordinates z and z'. Near the surface, z and z' are small and the vector $\boldsymbol{R} - \boldsymbol{R}'$ is almost parallel to the surface (see figure 1 top). This corresponds to the direction of surface phonon propagation. The situation differs for bulk thermal excitations where $\boldsymbol{R} - \boldsymbol{R}'$ does not have any preferential direction.

In particular, for the limit of small z, z' we get from (9) and (10) the ratio between the surface correlation function and the bulk one:

$$\frac{Y^S}{Y^V} = \frac{C_{11}^2 + C_{44}^2}{C_{11}^2 - C_{44}^2}. \tag{11}$$

For GaAs this ratio is equal to 1.67 (we have taken the values $C_{11} = 11.9 \times 10^{10}$ Pa, $C_{44} = 5.95 \times 10^{10}$ Pa for a GaAs crystal [16]). This means that the surface correlation function exceeds the volume one in the limit of small z, z'. In contrast, for the bulk case, $z, z' \gg \lambda_{ac}$, the surface contribution is negligible, i.e. Y^S/Y^V goes to zero. Of course, for both cases the z, z' are limited by the penetration depth ($L_{pen} = 1/(2k \operatorname{Im} \sqrt{\alpha_i^2 + \chi_0})$) of the probing x-rays. Variation of the x-ray penetration depth can be realized in a GID experiment, so bulk and surface excitations can be probed. Further, using the relationship (7) in the long-wavelength approximation considered, we can estimate the surface contribution to the imaginary part of the susceptibility, which is similar to (11).

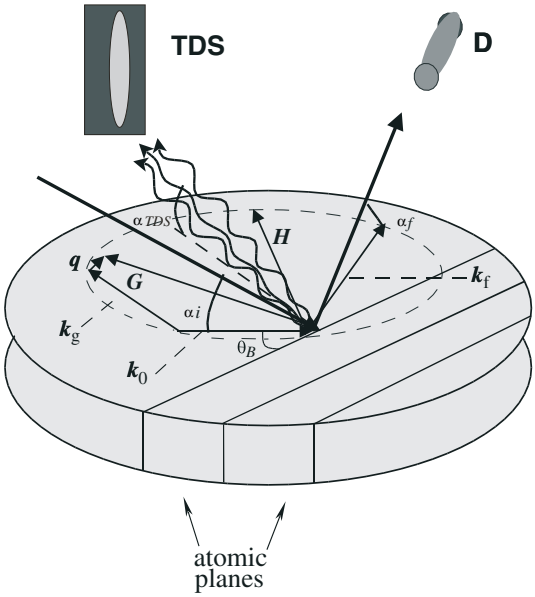

Figure 2. The schematic set-up of the TDS experiment and the inelastic scattering geometry in reciprocal space for GID conditions; TDS and D are the inelastically scattered and diffracted beam detectors, respectively.

3. Experiment

The GID experiment was carried out at the beamline ID1 of the European Synchrotron Radiation Facility (Grenoble, France). The beamline is especially designed to achieve a large tunable energy range, good energy resolution and a low background. The experiments were performed using a perfect GaAs single crystal with a flat polished surface in [0 0 1] orientation. A schematic layout of the experimental set-up is shown in figure 2. The incident beam strikes the sample surface at an angle α_i. The crystal is rotated around the surface normal to excite the reflection $\boldsymbol{H} = (2\,2\,0)$ as a main reflection at an in-plane scattering angle $\theta = \theta_B$. At the same time, TDS is observed in the vicinity of two additional reciprocal-lattice points $\boldsymbol{G} = (10\,2\,0)$ and $\boldsymbol{G} = (12\,0\,0)$ for the energy 15.9 keV (critical angle $\alpha_c = 0.16°$). These conditions correspond to a weakly excited triple-wave diffraction with two dynamical diffraction vectors $\boldsymbol{H}$ and $\boldsymbol{G}$. The exact triple-point position can be found at an energy of 15.81 keV, where both diffraction vectors $\boldsymbol{H}$ and $\boldsymbol{G}$ lie exactly on the same Ewald sphere. The distance between the reciprocal-lattice vector $\boldsymbol{G}$ and the Ewald sphere (see figure 2) can be varied by slightly changing the energy ΔE. For a small variation of the energy this distance equals the length of the phonon wavevector $\boldsymbol{q}$. Since we are interested in the contribution of the long-wavelength excitations of acoustic phonons, this distance in k-space was chosen to be $\boldsymbol{q} \cong 0.05$ Å^{-1}, which corresponds to $\lambda \cong 12$ nm. A similar experimental situation for the GaAs crystal was considered in the work [5] for conventional Bragg diffraction.

In our experiment two detectors were used simultaneously: a scintillation detector for the elastically scattered beam at $\boldsymbol{H} = (2\,2\,0)$ and a position-sensitive detector (PSD) for the inelastically scattered beam close to $\boldsymbol{G}$. The advantage of using the PSD is that for a given angle of incidence α_i the TDS signals can be detected for different exit angles α_{TDS} simultaneously, i.e. from different information depths [9]. Unfortunately, the TDS signal was too weak

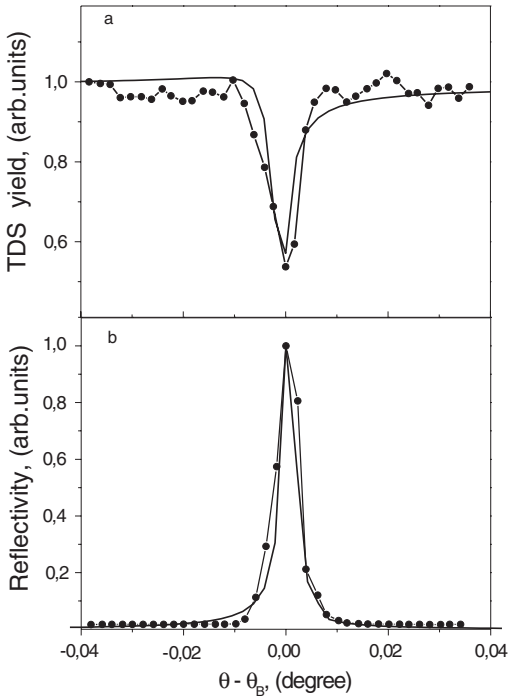

Figure 3. Experimental and calculated reflectivity curves for the GaAs (2 2 0) and TDS yield near the reciprocal-lattice vector (12 0 0) as a function of the deviation from the exact Bragg position θ_B for the angle of incidence $\alpha_i = 0.17°$.

(100 counts per 10 s) for exploiting the α_{TDS}-distribution. Therefore surface and bulk signals were registered by tuning α_i only. To do this, 480 PSD channels were collected simultaneously, which corresponds to an integration over an angular range of $0° \leqslant \alpha_{TDS} \leqslant 2.4°$. Inelastically scattered photons were detected starting from $\alpha_i = 0.1°$. In general, it is necessary to separate Compton scattering from the total inelastically scattered signal. The intensity of the Compton scattering depends on the scattering object and the angle between the incident and inelastically scattered beams. These angles were equal to 89.8° and 112.5° at the reciprocal-lattice points $\boldsymbol{G} = (10\ 2\ 0)$ and (12 0 0), respectively. In the present experiment, the Compton peak disappeared at both reciprocal-lattice points due to the geometric conditions.

Figure 3 shows experimental data and results of the calculations of the reflectivity (2 2 0) and the total TDS yield (the sum of surface and bulk TDS) near the reciprocal-lattice point $\boldsymbol{G} = (12\,0\,0)$. The calculation of the total TDS yield was performed using equations (1)–(10). The TDS curve displays a minimum at the scattering angle θ where the reflectivity curve has a maximum. This result has a simple physical explanation. In the angular region of dynamical scattering, x-rays do not penetrate deeper than the extinction depth L_{ex} [11]. Therefore TDS can be excited only from this depth. In conventional Bragg geometry this dip was investigated in a number of works [4, 6, 10] for bulk thermal excitations. However, in GID diffraction one can see (figure 4) that the depth of the dip varies with α_i. Moreover, the surface part dominates up to a penetration depth of 10 nm; i.e. for $\alpha_i = 0.12°$ we mainly register the surface signal. Experimental data and results of calculations for the surface and bulk TDS yields near the reciprocal-lattice point $\boldsymbol{G} = (10\ 2\ 0)$ are shown in figure 4. Four different incident angles are considered. Angles $\alpha_i = 0.12°$, 0.145°, 0.17° and 0.2° correspond to a penetration depth of

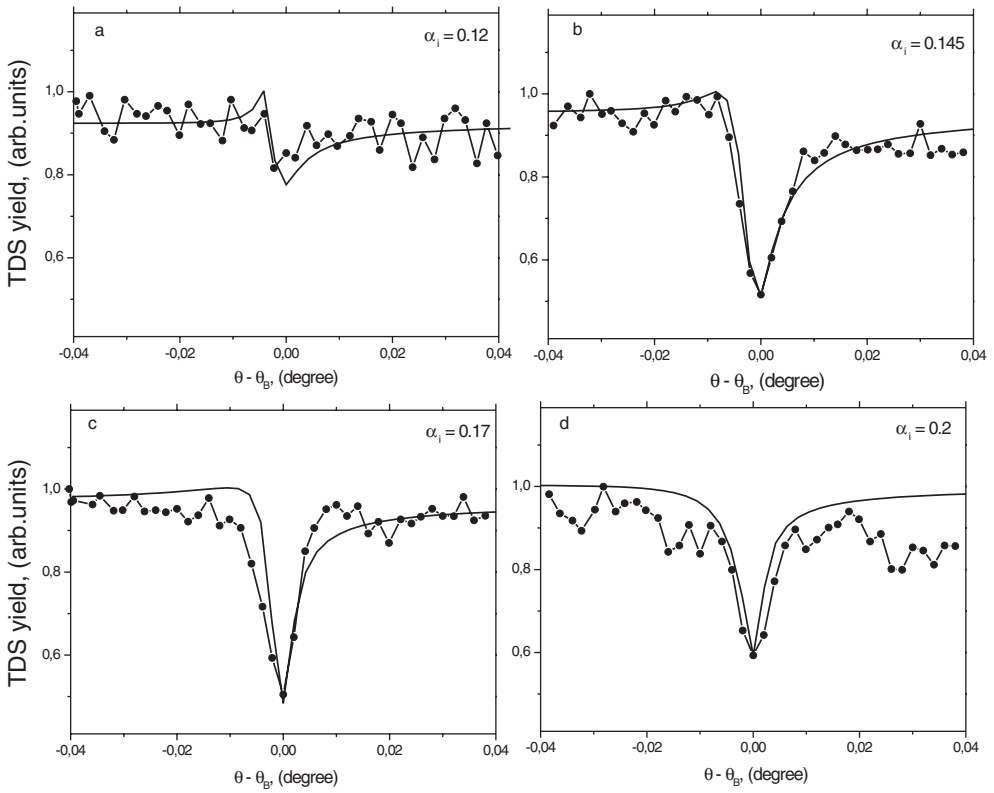

Figure 4. Experimental and calculated curves of the TDS yield as a function of the deviation from the exact Bragg position θ_B near the reciprocal-lattice vector (10 2 0) for different angles of incidence α_i.

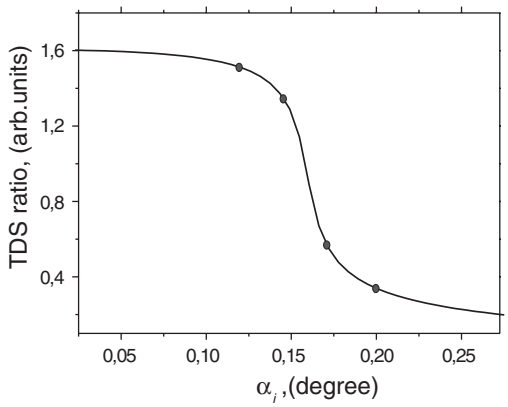

Figure 5. The surface and bulk TDS ratio $\kappa^S(\mathrm{TDS})/\kappa^V(\mathrm{TDS})$ as a function of the angle of incidence α_i. Filled circles indicate angles at which the experiment shown in figure 4 was performed.

x-rays $L_{pen} = 6$, 10, 50 and 110 nm, respectively. From the TDS geometry considered and equation (7), it follows that $\mathrm{Im}[\chi_{00}(\mathrm{TDS})] \approx \mathrm{Im}[\chi_{hh}(\mathrm{TDS})] \approx \mathrm{Im}[\chi_{0h}(\mathrm{TDS})]$ if scattering takes place in the vicinities of the reciprocal-lattice vector $\boldsymbol{G}[10\,2\,0]$. Therefore the shape of the

TDS yield curve is generated by nearly equal contributions of these three terms (corresponding to the direct, diffracted and interfering beams).

From the total TDS data obtained (see figure 4) and using equations (1)–(10), one can estimate the TDS ratio $\kappa^S(\mathrm{TDS})/\kappa^V(\mathrm{TDS})$ between the surface and the bulk TDS. In figure 5 we show the surface and bulk TDS yield ratio as a function of the incident angle α_i. This ratio definitely exceeds unity for the angles of incidence $\alpha_i \leqslant \alpha_c$. For the angles $\alpha_i = 0.12°$ and $0.145°$ (at which measurements were made in the present experiment, with the results shown by filled circles in figure 5) this ratio is equal to 1.5 and 1.3. In contrast, for the angle $\alpha_i = 0.2°$ it is only 0.3. So we may conclude that surface effects in the inelastic scattering of x-rays can play an important role under GID conditions.

4. Conclusions

In this paper we have shown that surface effects in the inelastic scattering of x-rays excited by thermal phonons are measurable under GID conditions. We have investigated the TDS yield for various angles of incidence and have considered both surface and bulk thermal excitations. Our findings can be effectively described in the framework of the general Green function formalism. The results imply that under GID conditions the contributions of surface excitations to inelastically scattered x-rays become comparable to or even exceed the bulk contributions. Of course, one has to note that the surface effects are very sensitive to the perfection of the crystal under investigation and, in particular, to the quality of the crystal surface. For doped GaAs crystals, for example, we found additional features in the yield of the diffuse scattering curves that are not seen for the perfect crystal. What is also interesting is that these curves were more sensitive to the imperfections of the crystal surface than the diffracted ones. A detailed study of these effects could be an interesting project for the future.

Acknowledgments

This work was supported by DAAD. We would like to acknowledge the support given by the ID1 beamline staff at ESRF and Ferdinand-Braun-Institut für Höchstfrequenztechnic-Berlin for providing the samples.

References

[1] Lindenberg A M *et al* 2000 *Phys. Rev. Lett.* **84** 111
[2] Occelli F *et al* 2001 *Phys. Rev.* B **63** 224306
[3] Sondhauss P and Wark J S 2003 *Acta Crystallogr.* A **59** 7
[4] Spalt H, Zounek A, Dev B N and Materlik G 1988 *Phys. Rev. Lett.* **60** 1868
[5] Zounek A, Spalt H and Materlik G 1993 *Z. Phys.* B **92** 21
[6] Grigorian S A, Vartanyants I A and Kovalchuk M V 2001 *J. Phys. D: Appl. Phys.* A **34** 78
[7] Vartanyants I A, Grigorian S A and Kovalchuk M V 2001 *Phys. Status Solidi* b **225** 401
[8] Cowan P L, Brennan S, Jach T, Bedzik M J and Materlik G 1986 *Phys. Rev. Lett.* **57** 2399
[9] Holy V, Pietsch U and Baumbach T 1999 *High Resolution X-ray Scattering from Thin Films and Multilayers (Springer Tracts in Modern Physics vol 149)* (Berlin: Springer)
[10] Afanas'ev A M and Azizian S L 1981 *Acta Crystallogr.* A **37** 125
[11] Vartanyants I A and Kovalchuk M V 2001 *Rep. Prog. Phys.* **64** 1009
[12] Pinsker Z G 1978 *Dynamical Scattering of X-Rays in Crystals* (Berlin: Springer)
[13] Afanas'ev A M and Melkonyan M K 1983 *Acta Crystallogr.* A **39** 207
[14] Afanas'ev A M and Kagan Yu 1968 *Acta Crystallogr.* A **24** 163
[15] Wooster W A 1962 *Diffuse X-Ray Reflections from Crystals* (Oxford: Clarendon)
[16] Berger L I 1997 *Semiconductor Materials* (Boca Raton, FL: Chemical Rubber Company Press)